Modeling the Electrophysiological Impact of Chagas Disease on the Heart

Angela M Gómez[1], Catalina Tobón[1], Juan P Ugarte[2], Javier Saiz[3]

[1] MATBIOM, Universidad de Medellín, Medellín, Colombia
[2] GIMSC, Universidad de San Buenaventura, Medellín, Colombia
[3] Ci2B, Universitat Politècnica de València, Valencia, Spain

Abstract

Chagas disease, caused by Trypanosoma cruzi, affects millions in Latin America and often leads to fatal cardiac arrhythmias, though its electrical mechanisms remain poorly understood. Using computational models of human ventricular myocytes and 2D tissue, this study simulated the progressive effects of Chagas-related remodeling (acute, intermediate, and chronic stages). Our results show that combined chronic alterations, particularly reduced L-type calcium current, produce marked arrhythmogenic changes, including shortened action potentials, progressive attenuation of restitution properties, and slower conduction. This in-silico approach provides insights into how disease progression alters cardiac electrophysiology and may guide improved diagnosis, risk stratification, and therapy.

1. Introduction

Chagas disease, caused by *Trypanosoma cruzi*, affects around 10 million people, primarily in Latin America countries where the disease is endemic [1], [2]. Its acute and chronic phases are unpredictable and may result in fatal myocarditis [3], with sudden death due to ventricular arrhythmias in up to 60% of cases [4], [5]. A significant proportion of these deaths occur among young adults of working age who may also experience disabling conditions.

The underlying electrophysiological remodeling remains poorly understood, and current treatment relies on non-specific guidelines without disease-specific validation, being more effective at early ages or in recently infected individuals [6], [7].

Studies on cardiomyocytes during acute and chronic stages indicate reduced calcium influx due to attenuated L-type calcium channels (I_{CaL}), compromising calcium release from the sarcoplasmic reticulum via ryanodine receptors [8]. During diastole, impaired calcium reuptake leads to cytosolic calcium overload [9]. The transient outward potassium current (I_{to}) is markedly reduced [10], while the slow delayed rectifier potassium current is increased [11]. Electrical coupling is also disrupted by decreased connexin-43 expression [12].

2. Methods

In this study, we used the O'Hara mathematical model of human ventricular myocytes [13] and a 2D tissue model to analyze the individual and combined effects of Chagas-related alterations on cardiac electrophysiology and conduction.

2.1. Ventricular myocyte and 2D tissue models with Chagas-induced remodeling

Based on experimental data on *T. cruzi* invasion [9]–[12], simulations were performed to represent the acute, intermediate, and chronic stages of Chagas disease, corresponding to increasing degrees of remodeling. Specifically, the L-type calcium current (I_{CaL}), the transient outward potassium current (I_{to}), and the sarcoplasmic reticulum calcium release flux (J_{rel}) were reduced by 25%, 50%, and 75%, respectively, while the slow delayed rectifier potassium current (I_{Ks}) and the intracellular calcium concentration ($[Ca^{2+}]_i$) were increased by the same proportions.

The modified single-cell model was integrated into a 2D model of human ventricular tissue to assess the impact of Chagas-induced alterations on cardiac conduction. We developed a 6 x 6 cm square mesh, composed of 192 x 192 elements, with a spatial discretization of 312.5 μm. An isotropic tissue was considered. The following equation describes the propagation of the action potential in the 2D domain:

$$K\left(\frac{\partial^2}{\partial x^2}+\frac{\partial^2}{\partial y^2}\right)V_m = C_m\frac{\partial V}{\partial t} + I_{ion} + I_{st}\ , \quad (1)$$

where V_m is the membrane potential, I_{ion} is the sum of the transmembrane ionic currents corresponding to each model, I_{st} represents the external stimulation and C_m designates the membrane capacitance.

The diffusion coefficient K was adjusted to obtain a realistic conduction velocity of 43.5 cm/ under control conditions. To represent conduction alterations during the acute, intermediate, and chronic stages of Chagas disease, K was reduced by 10%, 17.5%, and 25%, respectively. The

integration time step was set to 0.01 ms.

2.2. Stimulation protocols

At the single cell level, a S1-S1 stimulation protocol was applied. This consisted of a train of 10 rectangular pulses with a duration of 0.5 ms and amplitude of -80 μA/μF, delivered at a basic cycle length (BCL) of 1000 ms. The action potential duration at 90% of the repolarization (APD_{90}) and the different ionic currents were measured on the 10th beat. To construct the action potential duration (APD) restitution curve, cells were paced with a single train of 10 stimuli (S1), starting at a BCL of 1000 ms.

The APD_{90} from the 10th beat at 1000 ms was taken as the control value. The BCL was then progressively shortened within the same train until the 10th action potential failed to be generated. The restitution curve was then constructed by plotting APD_{90} as a function of BCL. To quantify restitution properties, the curves were fitted with a mono-exponential function, from which the steady-state APD (APD_{ss}), amplitude of adaptation, and time constant were extracted. The maximal slope of the restitution curve was also calculated as an indicator of dynamic stability.

At the 2D level, a cross-field S1-S2 stimulation protocol was applied, where S1 consisted of a train of 10 flat stimuli delivered at a BCL of 1000 ms and applied to the left end of the tissue, and S2 is a premature stimulus applied to the top of the tissue when the repolarization wavefront generated by S1 exceeds half the domain. The time elapsed between the application of S1 and S2 is called the coupling interval.

Conduction velocity (CV) was computed as the distance between two measurement points (cells 48 and 144 in the middle of the tissue) divided by the activation-time difference. Wavelength was estimated as $\lambda = CV \times APD_{ss}$, where APD_{ss} approximates effective refractory period (ERP).

3. Results

Preliminary results suggest that *T. cruzi* induces electrophysiological modifications closely associated with arrhythmogenic processes.

3.1. Cellular level

The experimentally reported effects of Chagas disease were evaluated individually and in combination across its three stages: acute, intermediate, and chronic. Under control conditions, the APD_{90} measured at the tenth action potential was 265 ms. The individual effect of *T. cruzi* on I_{CaL} produced an APD_{90} reduction of 6.4%, 13.2%, and 22.6% in the acute, intermediate, and chronic stages, respectively. The effect on I_{to} resulted in the loss of phase 1 of the action potential and an APD_{90} reduction of 1.5%, 2.3%, and 2.6% in the acute, intermediate, and chronic stages, respectively. The effect on I_{Ks} led to an APD_{90} reduction of 2.6% and 3.8% in the intermediate and chronic stages, respectively, while no appreciable change was observed in the acute stage. The effect on J_{rel} did not alter APD_{90} at any stage. Finally, the effect on $[Ca^{2+}]_i$ produced an APD_{90} reduction of 1.9% only in the chronic stage, with no appreciable changes in the acute and intermediate stages.

When all effects were combined, APD was reduced by 7%, 14%, and 22% in the acute, intermediate, and chronic stages of Chagas disease, respectively. Figure 1 illustrates the action potential, I_{CaL}, I_{to}, I_{Ks}, and J_{rel} under control conditions and with the combined effects of Chagas disease across these three stages. The most pronounced alterations were observed in the chronic stage, with I_{CaL} changes contributing most significantly.

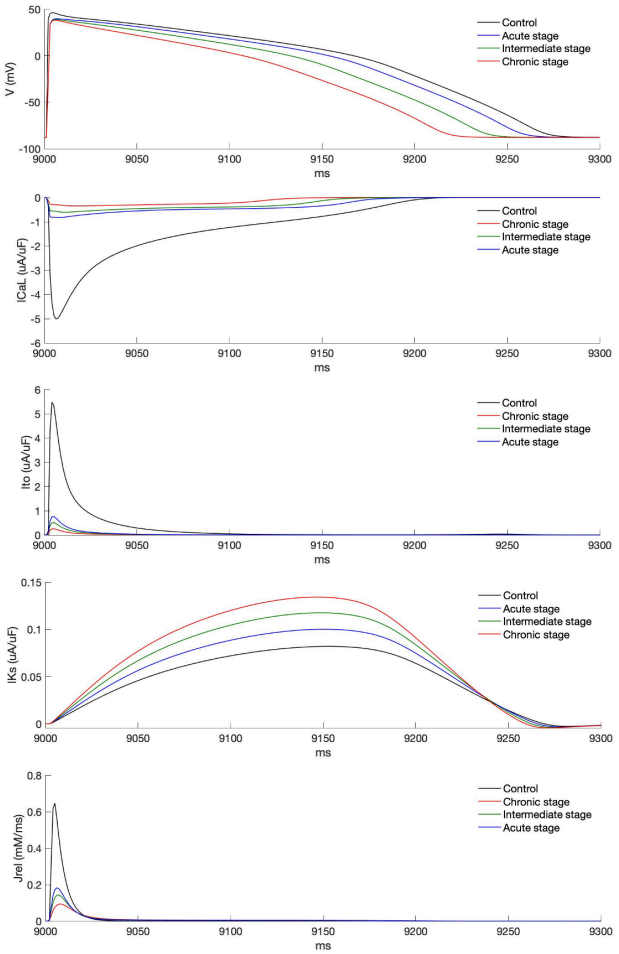


Figure 1. Action potential, I_{CaL}, I_{to}, I_{Ks}, and J_{rel} in control conditions and under the combined effects of Chagas disease during acute, intermediate, and chronic stages, obtained from the ventricular cell model.

Figure 2 shows the APD restitution curves in control, acute, intermediate, and chronic stages of Chagas disease. Analysis of restitution curves revealed that the maximal slope remained below 1 in all conditions (control: 0.125; acute: 0.132; intermediate: 0.106; chronic: 0.092), indicating that restitution alone is unlikely to induce alternans. Notably, maximal slope showed a slight increase in the acute stage, followed by a progressive decline towards the chronic stage. Exponential fitting of APD demonstrated a progressive reduction in the APD_{ss} (274.2 ms in control vs. 209.7 ms in chronic), as well as in the amplitude of adaptation (73.9 to 52.5) and the time constant (348.9 to 269.1 ms). These results indicate a gradual shortening of repolarization, accompanied by faster but less pronounced adaptation to changes in cycle length.

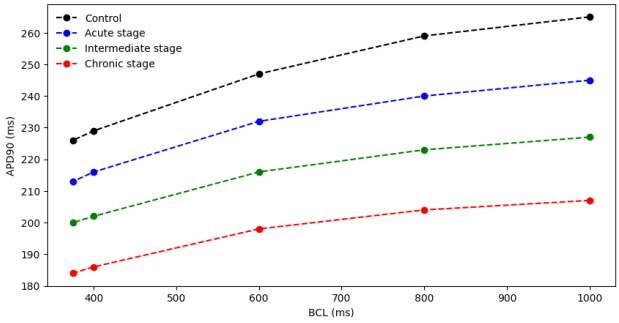


Figure 2. APD restitution curves in control, acute, intermediate, and chronic stages of Chagas disease.

Collectively, the data suggest that Chagas disease progressively alters restitution dynamics, with the chronic stage characterized by markedly APD shortened and attenuated restitution properties. While the restitution slope remains below 1, thereby reducing the likelihood of alternans, the overall shortening of APD and reduced adaptation reserve provide a substrate more prone to reentry and arrhythmogenic activity.

3.2. Tissue level

In 2D human ventricular tissue, the CV was 43.5 cm/s in control conditions. Under combined electrophysiological alterations characteristic of chronic Chagas disease, CV decreased to 34.6 cm/s (20.4%).

Using APD as a surrogate for ERP, the wavelength decreased from 11.9 cm (control) to 7.3 cm (chronic), representing a reduction of 38.7%. Thus, the combined slowing of conduction and APD shortening substantially reduced the excitation wavelength, creating a substrate more favorable to reentrant arrhythmias. Figure 3 shows the reentrant propagation dynamics in the 2D ventricular tissue model under the combined effects of the chronic stage of Chagas disease.

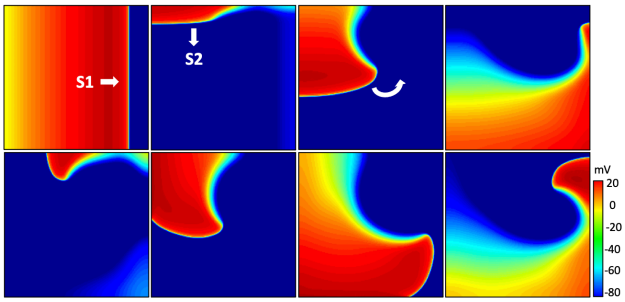


Figure 3. Reentrant propagation dynamics in the 2D ventricular tissue model under the combined effects of the chronic stage of Chagas disease.

4. Discussion

The results of this in-silico study show that the progression of Chagas disease is associated with a progressive APD shortening, a decrease in the slope and amplitude of restitution curves, as well as conduction slowing and a significant reduction in excitation wavelength in simulated human ventricular tissue. These modifications generate an arrhythmogenic substrate consistent with the clinical manifestations observed in patients with chronic Chagas cardiomyopathy, particularly the high incidence of ventricular arrhythmias and sudden cardiac death [3]–[5].

At the cellular level, our findings confirm that the reduction in I_{CaL} is the main determinant of APD shortening, in agreement with experimental studies describing attenuated calcium influx in infected cardiomyocytes [8], [9]. The relatively smaller impact of changes in I_{to} and I_{Ks} suggests that although these currents contribute to electrical remodeling, their isolated effect cannot fully explain the marked repolarization changes. On the other hand, the progressive increase in $[Ca^{2+}]_i$ during advanced stages could contribute to intracellular calcium overload, as previously reported [9], promoting triggered activity.

Regarding restitution dynamics, this study shows that the maximal slope of the restitution curve remains below 1 under all conditions, reducing the likelihood of repolarization alternans as a primary mechanism of instability. However, the shortening of APD and the reduced adaptation capacity (lower amplitude and time constant) observed in chronic stages are consistent with an increased vulnerability to reentrant phenomena. This finding is relevant, as clinical studies have reported that patients with advanced disease often present sustained ventricular arrhythmias even in the absence of marked alternans [4], [9].

At the tissue level, the conduction slowing observed (≈20% CV reduction) and the subsequent decrease in wavelength by almost 40% are highly significant. The combination of shortened repolarization and impaired

conduction favors wavefront fragmentation and the perpetuation of reentrant circuits [5], [12]. In this context, the reduction in connexin-43 expression described in experimental infection models [12] may at least partially explain the conduction impairment represented in this computational model. Our findings support the hypothesis that alterations in electrical coupling are not merely a structural finding but actively contribute to arrhythmogenesis.

This work also provides evidence on the progression of electrophysiological changes from acute to chronic stages. While early alterations are relatively mild and limited to modest changes in APD and restitution, advanced stages show profound remodeling with effects on repolarization, conduction, and wavelength. This is consistent with the clinical course of Chagas cardiomyopathy, in which asymptomatic patients in early phases progress toward ventricular dilation, heart failure, and a high arrhythmic risk in chronic stages [3], [7].

This study has limitations, as it relied on an averaged ventricular myocyte model without cellular heterogeneity or structural remodeling (fibrosis, inflammation, anatomical changes), which are central to chronic Chagas cardiomyopathy. In addition, only 2D tissue simulations were performed, and future 3D studies could provide a more realistic view. Despite these constraints, our findings highlight I_{CaL} remodeling and impaired cell-to-cell coupling as key drivers of the arrhythmogenic substrate in Chagas disease. Computational modeling thus offers valuable insights into disease mechanisms and may guide the development of targeted diagnostic and therapeutic strategies.

5. Conclusion

This in silico study shows that Chagas disease-related ionic remodeling, primarily characterized by reduced I_{CaL} and impaired coupling, promotes shortened action potentials, slow conduction, and reduced wavelength, thereby creating a proarrhythmic substrate. Such insights gained through computational modeling provides information that could improve diagnosis, risk assessment, and targeted therapies in Chagas cardiomyopathy.

Acknowledgments

This work was partially funded by the University of Medellin through Project 1351; by the Bicentennial Doctoral Excellence Program 2019 of MINCIENCIAS, Colombia; by the *Dirección General de Política Científica* of the Generalitat Valenciana, Spain PROMETEO 2024 CIPROM/2023/14; and by grant PID2022-140553OB-C41 funded by MICIU/AEI/10.13039/501100011033 and by ERDF/EU.

References

[1] C. P. Benziger, G. A. L. do Carmo, and A. L. P. Ribeiro, "Chagas cardiomyopathy," *Cardiol. Clin.*, vol. 35, no. 1, pp. 31–47, 2017.

[2] E. M. Cronin *et al.*, "2019 HRS/EHRA/APHRS/LAHRS expert consensus statement on catheter ablation of ventricular arrhythmias: executive summary," *EP Eur.*, vol. 22, no. 3, pp. 450–495, Mar. 2020.

[3] A. Rassi, A. Rassi, and J. A. Marin-Neto, "Chagas disease," *Lancet*, vol. 375, no. 9723, pp. 1388–1402, Apr. 2010.

[4] R. B. Bestetti and A. Cardinalli-Neto, "Sudden cardiac death in chagas' heart disease in the contemporary era," *Int. J. Cardiol.*, vol. 131, no. 1, pp. 9–17, 2008.

[5] A. Rassi, A. Rassi, and S. G. Rassi, "Predictors of mortality in chronic chagas disease: a systematic review of observational studies," *Circulation*, vol. 115, no. 9, pp. 1101–1108, 2007.

[6] C. M. Carneiro *et al.*, "Experimental and clinical treatment of chagas disease: a review," *Am. J. Trop. Med. Hyg.*, vol. 97, no. 5, pp. 1–33, 2017.

[7] A. L. Ribeiro, M. P. Nunes, M. M. Teixeira, and M. O. C. Rocha, "Diagnosis and management of chagas disease and cardiomyopathy," *Nat. Rev. Cardiol.*, vol. 9, no. 10, pp. 576–589, 2012.

[8] D. Roman-Campos *et al.*, "Cardiomyocyte dysfunction during the chronic phase of chagas disease," *Mem. Inst. Oswaldo Cruz*, vol. 108, no. 2, pp. 243–245, Apr. 2013.

[9] D. Roman-Campos, J. A. Marin-Neto, A. Santos-Miranda, A. D. Nathan Kong, and A. J. Rassi, "Arrhythmogenic manifestations of chagas disease: perspectives from the bench to bedside," *Circ Res*, vol. 134, no. 10, pp. 1379–1397, 2024.

[10] L. M. Pacioretty, S. C. Barr, W. P. Han, and R. F. Gilmour, "Reduction of the transient outward potassium current in a canine model of chagas' disease.," *Am. J. Physiol.*, vol. 268, no. 3 Pt 2, pp. H1258--H1264, 1995.

[11] E. H. Medei *et al.*, "Antibodies with beta-adrenergic activity from chronic chagasic patients modulate the QT interval and M cell action potential duration," *Europace*, vol. 10, no. 7, pp. 868–876, May 2008.

[12] D. Adesse, L. R. Garzoni, H. Huang, H. B. Tanowitz, M. de Nazareth Meirelles, and D. C. Spray, "Trypanosoma cruzi induces changes in cardiac connexin43 expression," *Microbes Infect.*, vol. 10, no. 1, pp. 21–28, Jan. 2008.

[13] T. O'Hara, L. Virág, A. Varró, and Y. Rudy, "Simulation of the undiseased human cardiac ventricular action potential: model formulation and experimental validation," *PLoS Comput. Biol.*, vol. 7, no. 5, p. e1002061, May 2011.

Address for correspondence:
Catalina Tobón Zuluaga
Cra. 87 #30-65, Medellín
ctobon@udemedellin.edu.co